# Mutual promotion between aerosol particle liquid water and particulate nitrate enhancement leads to severe nitrate-dominated particulate matter pollution and low visibility

Yu Wang[1,2,a], Ying Chen[3,a], Zhijun Wu[1,4,5,*], Dongjie Shang[1], Yuxuan Bian[6], Zhuofei Du[1,b], Sebastian H. Schmitt[4,7,c], Rong Su[1,d], Georgios I. Gkatzelis[4,7,e,f], Patrick Schlag[4,7,g], Thorsten Hohaus[4,7], Aristeidis Voliotis[2], Keding Lu[1,4,5], Limin Zeng[1,4], Chunsheng Zhao[8], Rami Alfarra[2,9], Gordon McFiggans[2], Alfred Wiedensohler[10], Astrid Kiendler-Scharr[4,7], Yuanhang Zhang[1,4,5], Min Hu[1,4,5]

[1]State Key Joint Laboratory of Environmental Simulation and Pollution Control, College of Environmental Sciences and Engineering, Peking University, Beijing 100871, China
[2]Centre for Atmospheric Science, School of Earth and Environmental Sciences, The University of Manchester, Manchester M13 9PL, UK
[3]Lancaster Environment Centre, Lancaster University, Lancaster, LA1 4YQ, UK
[4]International Joint Laboratory for Regional Pollution Control, 52425 Jülich, Germany, and Beijing 100871, China
[5]Collaborative Innovation Center of Atmospheric Environment and Equipment Technology, Nanjing University of Information Science and Technology, Nanjing 210044, China
[6]State Key Laboratory of Severe Weather, Chinese Academy of Meteorological Sciences, Beijing, 100081, China
[7]Institute for Energy and Climate Research, IEK-8: Troposphere, Forschungszentrum Jülich, 52425 Jülich, Germany
[8]Department of Atmospheric and Oceanic Sciences, School of Physics, Peking University, Beijing 100871, China
[9]National Centre for Atmospheric Science, School of Earth and Environmental Sciences, The University of Manchester, Manchester, M13 9PL, UK
[10]Leibniz Institute for Tropospheric Research, 04318 Leipzig, Germany

[a]These authors contribute equally to this work
[b]Now at Center for Urban Transport Emission Research & State Environmental Protection Key Laboratory of Urban Ambient Air Particulate Matter Pollution Prevention and Control, College of Environmental Science and Engineering, Nankai University, Tianjin, 300071, China
[c]Now at TSI GmbH, 52068 Aachen, Germany
[d]Now at Guangdong Science and Technology Monitoring and Research Center, Guangzhou 510033, China
[e]Now at NOAA Earth Systems Research Laboratory, Boulder, Colorado 80305, United States
[f]Now at Cooperative Institute for Research in Environmental Sciences, Boulder, Colorado 80309, United States
[g]Now at Shimadzu Deutschland GmbH, 47269 Duisburg, Germany

*Correspondence to*: Zhijun Wu (zhijunwu@pku.edu.cn)

**Abstract.** As has been the case in North America and Western Europe, the $SO_2$ emissions substantially reduced in North China Plain (NCP) in recent years. A dichotomy of reductions in $SO_2$ and $NO_x$ concentrations result in the frequent occurrences of nitrate ($pNO_3^-$)-dominated particulate matter pollution over NCP. In this study, we observed a polluted episode with the particulate nitrate mass fraction in non-refractory $PM_1$ (NR-$PM_1$) up to 44% during wintertime in Beijing. Based on this typical $pNO_3^-$-dominated haze event, the linkage between aerosol water uptake and $pNO_3^-$ enhancement, further impacting on visibility degradation, have been investigated based on field observations and theoretical calculations. During haze development, as ambient relative humidity (RH) increased from ~10% up to 70%, the aerosol particle liquid water increased from ~1 μg/m$^3$ at the beginning to ~75 μg/m$^3$ at the fully-developed haze period. The aerosol liquid water further increased the aerosol surface area and volume, enhancing the condensational loss of $N_2O_5$ over particles. From the beginning to the fully-developed haze, the condensational loss of $N_2O_5$ increased by a factor of 20 when only considering aerosol surface area and volume of dry particles, while increasing by a factor of 25 considering extra surface area and volume due to water uptake. Furthermore, aerosol liquid water favored the thermodynamic equilibrium of $HNO_3$ into the particle phase under the supersaturated $HNO_3$ and $NH_3$ in the atmosphere. All above results demonstrated that the $pNO_3^-$ is enhanced by aerosol water uptake with elevated ambient RH during haze development, in turn, facilitating the aerosol taking up water due to the hygroscopicity of particulate nitrate salt. Such mutual promotion between aerosol particle liquid water and particulate nitrate enhancement can rapidly degrade air quality and halve visibility within one day. Reduction of nitrogen-containing gaseous precursors, e.g., by control of traffic emissions, is essential in mitigating severe haze events in NCP.

# 1 Introduction

Aerosol particle hygroscopicity plays an important role in air quality deterioration and cloud formation (Yu, 2009;Fitzgerald, 1973;Kreidenweis and Asa-Awuku, 2014;Wang and Chen, 2019;McFiggans et al., 2006) and can also directly influence aerosol measurements (Chen et al., 2018a). In atmospheric environments influenced by anthropogenic activities, particulate secondary inorganic compounds are often dominated by particulate sulfate and nitrate (Heintzenberg, 1989), which originate from the oxidation of sulfur dioxide ($SO_2$) and nitrogen oxides ($NO_x$) via multiple chemical pathways (Calvert et al., 1985;Cheng et al., 2016;Wang et al., 2016;Gen et al., 2019a, b). The abundance of secondary inorganic components is one of the most important factors determining particle hygroscopicity (Swietlicki et al., 2008), thereby governing the aerosol liquid water content under ambient moist conditions. Increased aerosol particle liquid water could accelerate secondary inorganic and organic aerosol formation by decreasing the kinetic limitation of mass transfer of gaseous precursors and providing more medium for multiphase reactions (Mozurkewich and Calvert, 1988;Cheng et al., 2016;Wang et al., 2016;Ervens et al., 2011;Kolb et al., 2010).

Sulfuric acid ($H_2SO_4$) is formed from the oxidation of $SO_2$ via gaseous and multiphase reactions. $H_2SO_4$ is subsequently fully or partly neutralized by gaseous $NH_3$ taken up on particles, resulting in the formation of $(NH_4)_2SO_4$ and / or $NH_4HSO_4$. Any remaining $NH_3$ is available to neutralize $HNO_3$ to form particulate $NH_4NO_3$ (Seinfeld. and Pandis., 2006) (and further excess $NH_3$ can neutralize any available HCl to form particulate $NH_4Cl$). Over the past several decades, substantial efforts have reduced emissions of both $SO_2$ and $NO_x$ improving the local and regional air quality all over the world.

For example, $SO_2$ and $NO_x$ emissions were reduced by 82% and 54% in the majority of European Environment Agency member countries between 1990 and 2016 (https://www.eea.europa.eu/data-and-maps/indicators/main-anthropogenic-air-pollutant-emission s/assessment-4). In consequence, an increasing trend of $NO_3^-/SO_4^{2-}$ molar ratio was observed in long-term measurements at Leipzig, Germany (Spindler et al., 2004) and at some other European sites from the European Monitoring and Evaluation Programme (EMEP) (Putaud et al., 2004).

In the recent years, China has also managed to reduce $SO_2$ emissions by 75% during 2007~2015 (Li et al., 2017a) and declined by ~15.1% per year during 2013~2017 (Vu et al., 2019), whereas $NO_x$ emissions declined only by ~10% between 2011 and 2015 (de Foy et al., 2016) and by ~ 4.3% per year during 2013~2017 (Vu et al., 2019). The strict emission control reduced the $PM_{2.5}$ mass concentration and the corresponding chemical components in China significantly (Vu et al., 2019). The annual mean $PM_{2.5}$ mass loading decreased by 39.6% during 2013~2017 in Beijing-Tianjin-Hebei region, and the $SO_4^{2-}$ and $NO_3^-$ mass concentrations in the $PM_{2.5}$ declined by 40% and 34% respectively during 2015~2017 in Beijing (Vu et al., 2019). However, $NH_3$ emissions have been observed by satellites to increase by ~30% from 2008 to 2016 over the North China Plain (NCP) (Liu et al., 2018). The faster reduction rate of $SO_2$ than $NO_x$ emissions in conjunction with elevated $NH_3$ level, made it reasonable of switching dominant inorganic component in fine aerosol particles from sulfate to nitrate in the recent years similar like European countries (Sun et al., 2015;Hu et al., 2017;Hu et al., 2016;Wu et al., 2018;Guo et al., 2014;Huang et al., 2014;Huang et al., 2010;Ge et al., 2017;Xu et al., 2019a;Xie et al., 2019;Li et al., 2018). Field measurements in Beijing show that annually averaged $NO_3^-/SO_4^{2-}$ molar ratio of NR-$PM_1$ (non-refractory $PM_1$) in 2012 (1.3~1.8) (Sun et al., 2015) has significantly increased

compared to that in 2008 (0.9~1.5) (Zhang et al., 2013). Comparably, the $NO_3^-/SO_4^{2-}$ molar ratio of $PM_{2.5}$ in Beijing increased substantially, from 1.5 before 2013 to 3.33 in 2017 (Xu et al., 2019a).

Over the NCP region, heavy haze events are typically associated with enhanced ambient RH levels. This leads to an increased aerosol liquid water content (Wu et al., 2018), which will enhance the particulate nitrate formation by increasing the reactive uptake of precursors and the thermodynamic equilibrium of ammonium nitrate (Cheng et al., 2016;Wang et al., 2016;Wang et al., 2017;Yun et al., 2018;Yue et al., 2019). To date, few studies reported aerosol liquid water content over NCP region (Wang et al., 2018;Bian et al., 2014;Cheng et al., 2016;Wu et al., 2018;Ge et al., 2019). However, the observational and theoretical analysis of the relationship between particulate nitrate enhancement and associated liquid water during haze events in China has been infrequently reported (Wu et al., 2018).

In this study, a self-amplification effect between particulate nitrate and liquid water is demonstrated by examining a nitrate-dominated fine particle Beijing pollution episode. The facilitation of particulate nitrate enhancement by abundant aerosol liquid water is subsequently theoretically explored through the impacts of liquid water on thermodynamic equilibrium and heterogeneous reactions. Finally, the corresponding impacts on light extinction coefficient, and visibility degradation are estimated. These results improve our quantitative understanding of the development of haze events over the NCP and on formulating emission reduction strategies, as well as may also provide insights for other polluted regions.

# 2 Measurements and Methods

## 2.1 Location and instrumentation

Measurements were conducted within the framework of the BEST-ONE (Beijing winter finE particle STudy- Oxidation, Nucleation, and light Extinctions) field campaign from January 1 to March 5, 2016, at the Huairou site (40.42°N, 116.69°E), located in a rural environment, north of Beijing, China. Detailed information about the sampling site was described in Tan et al. (2018). A weather station (Met one Instrument Inc., USA) was performed to measure meteorological parameters (ambient RH, temperature, wind speed, wind direction) and detailed aerosol particle physical and chemical properties were recorded using a suite of state-of-the-science instrumentation. Hygroscopic growth factor (HGF) of sub-micrometer aerosol particles was measured using a Hygroscopicity-Tandem Differential Mobility Analyzer (H-TDMA, TROPOS, Germany) (Wu et al., 2011;Massling et al., 2011;Wang et al., 2018;Wu et al., 2016;Liu et al., 1978) and data retrieval followed the $TDMA_{inv}$ method in Gysel et al. (2009). The hygroscopicity parameter (κ) was estimated using by the κ-Köhler approach (Petters and Kreidenweis, 2007;Köhler, 1936). Size-resolved NR-$PM_1$ was recorded by an Aerodyne High-Resolution Time-of-Flight Aerosol Mass Spectrometry (HR-ToF-AMS, Aerodyne Research, Inc., USA) (DeCarlo et al., 2006). Regular calibration procedures followed as reported in Jayne et al. (2000) and Jimenez et al. (2003) and composition dependent correction followed as in Middlebrook et al. (2012). Gaseous $HNO_3$ and $NH_3$ were measured using Gas-Aerosol Collector (GAC) coupled with Ion Chromatography (IC) (Dong et al., 2012). Mass concentration of equivalent black carbon in aerosol particles (Petzold et al., 2013) was recorded by Multi Angle Absorption Photometer (MAAP, Model

5012, Thermo Fisher Scientific, USA) with a laser wavelength of 670 nm (Petzold and Schönlinner, 2004). Furthermore, particle number size distribution (PNSD) in the size range of 3 nm~10 μm was measured using a Mobility Particle Size Spectrometer (MPSS, Model 3776+3085 3775+3081, TSI, USA), following the recommendations described in Wiedensohler et al. (2012) and an Aerodynamic Particle Size Spectrometer (APS, Model 3021, TSI, USA) (Wu et al., 2008;Pfeifer et al., 2016). Detailed description on H-TDMA, HR-ToF-AMS and GAC-IC can be found in the supporting information.

### 2.2 Estimation of aerosol particle liquid water

Given the absence of direct liquid water measurement, size-resolved liquid water was calculated using the corresponding HGFs measured at RH=90% (50, 100, 150, 250, 350 nm in stokes diameter), PNSD data (3 nm~10 μm) and meteorological parameters (RH, T), following the method proposed in Bian et al. (2014), referred to below as H-TDMA-derived liquid water. Briefly, the measured PNSD with 57 size bins were fitted using a four-mode lognormal distribution. The classification of four modes and the fitting results are shown in Table S1 and Figure S4. Good agreement between measured values and fitted PNSD was achieved, which indicates the reliability of the four-mode lognormal fitting method. Based on four-mode lognormal fitting results, the particle number size distribution and number fractions of each mode can be obtained. It has been assumed that particles from the same mode have constant particle hygroscopicity (κ). Under the assumption of constant particle hygroscopicity in each mode (shown in Table S1), the $\kappa$ values for each mode ($\kappa_1$, $\kappa_2$, $\kappa_3$) can be calculated by Eq. [1] from the known

number fraction of fitted four modes and the $\kappa$ values of measured particle size from H-TDMA measurement.

$$\kappa = \sum_{i=1}^{4} \kappa_i f_i \quad [1]$$

Here, $\kappa_i$ and $f_i$ represent the $\kappa$ value and the particle number fraction of the i mode. Then, the calculated $\kappa$ values for each mode and the derived number fraction of each size bin were used to obtain the $\kappa$ distribution for each size bin. Figure S5 shows the comparison of calculated sized-resolved $\kappa$ distribution and the $\kappa$ measured by H-TDMA, the good agreement showed the reliability of the method. Then, based on $\kappa$-Kölher theory (Petters and Kreidenweis, 2007;Köhler, 1936), the size-resolved *HGF*s at ambient RH were calculated. Finally, liquid water of size-resolved particles can be derived by calculating the differentials between the dry and wet PNSD of aerosol particles in Eq. [2]:

$$\text{Liquid water} = \frac{\pi}{6} N_j D_{p,j}^3 \left( HGF\left(D_p, RH\right)^3 - 1 \right) * \rho_w \quad [2]$$

where j represents the bin number of measured PNSD, $N_j$ and $D_{p,j}$ represent the number concentration and the diameter of dry particles of the $j^{th}$ bin, respectively, while, *HGF* and $\rho_w$, are the hygroscopic growth factor of aerosol particles and water density (1 g/cm$^3$), respectively.

### 2.3 Condensation rate of trace gases

The condensation rate ($k$) of trace gases (dinitrogen pentoxide, $N_2O_5$, referred as k_$N_2O_5$) was calculated by the method of Schwartz (1986), shown in Eq. [3]. In order to illustrate the influences of the dry and wet PNSD due to water uptake on condensation rate of gases, the PNSD of the dry and wet

particles (obtained by applying the HGF estimated from H-TDMA-derived liquid water method) were used.

$$k = \frac{4\pi}{3}\int_0^{\infty}\left(\frac{r^2}{3D_g} + \frac{4r}{3C_g\gamma}\right)^{-1} r^3 \frac{dN}{dlogr} dlogr \qquad [3]$$

$$C_g = \sqrt{\frac{3RT}{M}} \qquad [4]$$

Where, $r$ represents radius of the particles, $D_g$ represents the binary diffusion coefficient evaluated following Maitland (1981) ($1.18*e^{-5}$ $m^2/s$). $C_g$ is the kinetic velocity of the gas molecules, calculated in Eq. [4]. Here, R and M are the ideal gas constant (8.314 $kg.m^2/mol/K/s^2$) and molar mass of the gas, respectively while T represents the ambient temperature. dN/dlogr is the number size distribution and γ is the uptake coefficient of the gas.

The uptake coefficient of $N_2O_5$ was estimated following the method proposed in Chen et al. (2018b) and Chang et al. (2016) and references therein. The influences of RH, temperature, multiple inorganic particle compositions, secondary organic aerosol (SOA) and primary organic aerosol (POA) are considered. The uptake suppression effect of $N_2O_5$ due to the presence of SOA was considered following the method in Anttila et al. (2006). Based on our source apportionment using Positive matrix factorization (SoFi tool, ME2, Francesco Canonaco, PSI), two oxygenated organic aerosol factors (OOA), usually interpreted as SOA, and three POA factors were determined. The fraction of SOA in the total organic aerosol (OA) was 60%~90% during the observed period, which is quite consistent with the results of a previous study in Beijing (Huang et al., 2014). Hence, 75% was used as the ratio of SOA/OA in our model to estimate the suppression effect of SOA on the uptake of $N_2O_5$ following the

work of Anttila et al. (2006). The reaction of chloride with $N_2O_5$ was not considered in this study due to its limited mass concentration (on average 5% of the $PM_1$ mass concentration during the marked haze period), which could cause minor uncertainty in the k_$N_2O_5$ calculation. The detailed information regarding the estimation $\gamma_{N2O5}$ is given in Chen et al. (2018b), and influences of different chemical components on $\gamma_{N2O5}$ is summarized in the Table 1 of Chen et al. (2018b).

### 2.4 Equilibrium of $NH_4NO_3$

The equilibrium dissociation constant of $NH_4NO_3$ ($Kp$) under dry conditions was calculated as a function of ambient temperature (Seinfeld. and Pandis., 2006) in the following Eq. [5].

$$lnK_p = 84.6 - \frac{24220}{T} - 6.1ln\left(\frac{T}{298}\right) \quad [5]$$

Taking into account the associated liquid water, the equilibrium vapor pressure of $HNO_3$ and $NH_3$ was calculated by employing the Extended-Aerosol Inorganic Model (E-AIM) Model II $H^+$ - $NH_4^+$ - $SO_4^{2-}$ - $NO_3^-$ - $H_2O$ (Clegg et al., 1998) using HR-ToF-AMS data, $NH_3$ from GAC-IC, and meteorological parameters (RH, T). In this calculation, a simplified ion pairing scheme was performed to ensure the ion balance of the input chemical composition following the method in Gysel et al. (2007).

### 2.5 Light extinction coefficient and visibility calculation

Size-resolved chemical composition of the NR-$PM_1$ from HR-ToF-AMS, mass concentration of equivalent black carbon from MAAP, PNSD data and the H-TDMA-derived liquid water were used to calculate light extinction coefficient (including light absorption and scattering) and visibility degradation of size-resolved particles by the Mie scattering theory described in Barnard et al. (2010).

Here, size-resolved equivalent black carbon mass concentration was inferred by the particle mass size distribution measurement from single particle soot photometer in PKUERS. The method of re-distribution of liquid water and HR-ToF-AMS data has been described in the supporting information (Text S1, HR-ToF-AMS introduction section). Thus, with the re-distributed datasets as the input of the Mie scattering theory, the light extinction coefficient for atmospheric particles in the absence and presence of liquid water with a size range of 100~2500 nm in stokes diameter can be derived. Due to lack of measurements on aerosol particle morphology and mixing state, we assume particles are spherical as described in Barnard et al. (2010). To perform Mie calculation, the complex reflective index of each component is given in Table 1 of Barnard et al. (2010) and references therein. This method shows good agreement with measurements in Mexico City and is consistent as the regional atmospheric chemistry model WRF-Chem. Here, Ext_550nm_wet and Ext_550nm_dry represent the calculated light extinction coefficient for particles in the presence and absence of liquid water at an incident light wavelength of 550 nm. The corresponding visibility degradation (VIS) for dry/wet particles was calculated from the light extinction coefficient following the Koschmieder Eq. [6].

$$VIS = \frac{3.912}{Ext\_550nm} \qquad [6]$$

# 3 Results and Discussion

## 3.1 Nitrate-dominated fine particulate matter pollution

Figure 1 illustrates a summary of chemical composition of NR-$PM_1$, ambient RH, size distribution and total aerosol particle liquid water, size distribution and total aerosol surface area concentration during

the period of February 29 to March 5, 2016 in the BEST-ONE campaign. During this period, polluted episodes occurred under stagnant meteorological conditions with low wind speed (Figure S6) and elevated ambient RH (Figure 1a). As marked 'haze period' in Figure 1, an obvious increase of NR-$PM_1$ was observed. The secondary inorganic components (sulfate, nitrate and ammonium) were dominant components of the NR-$PM_1$, accounting for up to 73% during the 'haze period'. Particularly, nitrate was the major contributor of the secondary inorganic components and accounted for up to ~44% of NR-$PM_1$ mass, while sulfate contributed for ~12% on average.

In the recent decade, severe haze events with high aerosol mass loading occurred frequently in Beijing during wintertime (Hu et al., 2016;Hu et al., 2017;Sun et al., 2014;Sun et al., 2015). To mitigate the air pollution, the Beijing government implemented strict emission controls. The total mass loading of particulate matter has reduced substantially in the recent years (http://sthjj.beijing.gov.cn/). With decreasing in PM mass concentration, the mass fraction of particulate nitrate during these haze events in Beijing enhanced substantially. In 2014, the highest fraction of nitrate in $PM_1$ was reported as ~20% and increased to ~35% in 2016 (Xu et al., 2019b), which is comparable to the ratio (44%) in this study. The particulate nitrate became more dominant in secondary inorganic compounds other than particulate sulfate with the air quality improvement over NCP.

As one of the main hydrophilic compounds in atmospheric aerosol particles, the ability of water uptake is comparable between deliquescent $(NH_4)_2SO_4$ and $NH_4NO_3$ particles with same sizes and ambient RH (Kreidenweis and Asa-Awuku, 2014;Wu et al., 2016), (http://umansysprop.seaes.manchester.ac.uk/). However, compared to $(NH_4)_2SO_4$, $NH_4NO_3$ particles have a lower deliquescence RH (62%, 298 K) than $(NH_4)_2SO_4$ (80%, 298 K) (Kreidenweis and Asa-Awuku, 2014) and easily liquefy (Li et al.,

2017b). In addition, $NH_4NO_3$ particles are semi-volatile, the co-condensation of semi-volatile compounds and water (Topping et al., 2013;Hu et al., 2018) could be significant. Therefore, the switching from sulfate-dominated to nitrate-dominated aerosol chemistry may impact on aerosol water uptake. The interaction between aerosol particle liquid water and particulate nitrate formation and visibility degradation should be reconsidered.

### 3.2 Mutual promotion between liquid water and particulate nitrate enhancement

Lu et al. (2019) conducted a box model to calculate the potential particulate nitrate formation during the same investigated period of the BEST-ONE project. They found out that $HNO_3$ from daytime photooxidation of $NO_2$ was the major source of the particulate nitrate (>75%), whereas the contribution of $N_2O_5$ pathway was lower than 25% (Lu et al., 2019). In the following discussion, the enhancement of particulate nitrate during the 'haze period' is elucidated by theoretical calculations of condensational loss rate of $N_2O_5$, and the thermodynamic equilibrium of $NH_4NO_3$ and $HNO_3$. In particular, the role of aerosol water uptake in particulate nitrate formation is comprehensively investigated.

$N_2O_5$ is an important gaseous precursor for particulate nitrate formation via its hydrolysis to form $HNO_3$ during nighttime (Brown et al., 2006). Liquid water can enhance aerosol surface areas and volumes, thereby increasing the available heterogeneous reacting medium. Across the development of 'haze period', the estimated liquid water increased from ~1 μg/m$^3$ at the beginning (March 2, 14:00~18:00 p.m.) to ~75 μg/m$^3$ when the haze was fully developed (March 4, 4:00~8:00 a.m.). The total surface area and volume concentrations of particles were increased by the liquid water by 2~3% at the beginning and by up to ~25 and ~40% in the fully-developed haze compared to the 'dry' values,

respectively (see Figure S7 and S8). Additionally, from the beginning to the fully-developed haze, the uptake coefficient of $N_2O_5$ was enhanced by a factor of 9 from 0.002 to 0.018, and the $k\_N_2O_5$ increased by a factor of 20 (dry particles); while, considering the increased particle surface area and volume due to water uptake, the respective value of enhanced $k\_N_2O_5$ was by a factor of 25 (Figure 2a). Apart from providing extra reacting medium, the abundant liquid water can liquefy the aerosol particles and may reduce any kinetic limitation of mass transfer for reactive gases (Koop et al., 2011;Shiraiwa et al., 2011) and impact thermodynamic equilibrium of semi-volatile compounds (Kulmala et al., 1993;Topping et al., 2013) to contribute to secondary aerosol formation. Our previous study provided the observational evidence that particles may have transitioned from the solid phase to the liquid phase as RH increased from 20% to 60% during wintertime in Beijing (Liu et al., 2017). In this study, the ambient RH increased from ~10% up to 70% during the haze period, suggesting a likely transition of particles from the solid to liquid phase. Such phase transition may facilitate particulate nitrate formation by increasing diffusion coefficients of dissolved precursors.

To illustrate the facilitation of particulate nitrate enhancement from $HNO_3$ in the presence of liquid water, we performed the theoretical calculation of equilibrium between particulate $NH_4NO_3$ and gaseous $NH_3$ and $HNO_3$ under dry and ambient conditions, respectively. The dissociation constant of $NH_4NO_3$ (*Kp*) in dry condition was calculated using Eq. [5] without considering the influence of the liquid water. As shown in Figure 3, the equilibrium *Kp* in the dry condition ranged from 0.06 (275.3 K) to 4.61 (291.5 K) $ppb^2$ during the 'haze period'. Taking account of the aerosol liquid water, the equilibrium vapor pressure of $HNO_3$ and $NH_3$ over particles was calculated by E-AIM Model II (www.aim.env.uea.ac.uk). Note that this calculation assumes negligible interaction between dissolved

organic components and the activity of $NO_3^-$. In the presence of aerosol associated water, the product of equilibrium vapor pressure of $NH_3$ and $HNO_3$ calculated from E-AIM was 10~60% lower than the equilibrium *Kp* in the dry condition during the marked 'haze period'. This means, the presence of aerosol liquid water changed the equilibrium and would favor the particulate nitrate enhancement. However, the aerosol particles didn't reach the equilibrium between particulate $NH_4NO_3$ and the gases ($NH_3$ + $HNO_3$) during the investigated period, as the measured product of the $NH_3$ and $HNO_3$ partial pressure (2.55~9.63 $ppb^2$) was supersaturated compared to the equilibrium values in both dry and deliquescent particles. In this case, the partitioning of gaseous $NH_3$ and $HNO_3$ in the atmosphere into the particle phase could be accelerated and leaded particulate nitrate enhancement as increasing of ambient RH. Owing to the nature of highly hydrophilic, the increased ammonium nitrate mass fraction leads to further water uptake. Such a mutual promotion of particulate nitrate and aerosol liquid water enhancement becomes more pronounced with the increasing pollution throughout the haze event owing to the simultaneously increasing ambient RH. Consistently, a significant co-increase of particulate nitrate and aerosol liquid water was observed during haze development as shown in Figure 4. At first, a steep increase of particulate nitrate in total nitrate mass ratio (from ~12% to ~98%) was observed as the aerosol liquid water enhanced up to ~20 $\mu g/m^3$. And then, the particulate nitrate mass kept increasing with further increase of aerosol liquid water. We observed that, ~98% of nitrate was present as particle phase when aerosol liquid water was higher than ~20 $\mu g/m^3$. The function between the particulate nitrate fraction in the total nitrate is given in Figure 4. It is worth noting that $N_2O_5$ hydrolysis during nighttime can contribute extra $HNO_3$ in the wet denuding method within GAC-IC system. This effect explains the slightly underestimation of the particulate fraction during nighttime when aerosol liquid

water is less than 10 μg/m$^3$ (Figure 4). However, the general consistency of this function between daytime and the nighttime (Figure 4) suggests a negligible influence of $N_2O_5$ interference on our analysis during the investigated period.

Except for aerosol liquid water, aerosol pH is also an important factor on the particulate nitrate formation, higher pH is favorable for the equilibrium of $HNO_3$ into the particle phase (Nah et al., 2018). pH of the fine aerosol particles was calculated by ISORROPIA II (Fountoukis and Nenes, 2007) during the investigated period. The model was running in 'forward mode' with chemical composition of NR-$PM_1$ ($NO_3^-$, $SO_4^{2-}$, $Cl^-$, $NH_4^+$) and gas precursors ($HNO_3$, HCl, $NH_3$) by GAC-IC as inputs. And the model was running in 'metastable mode', assuming no solid existed in the system. Generally, the fine aerosol particles became more acidic with pH dropping from ~8 down to ~4 when NR-$PM_1$ mass concentration increased from ~12 μg/m$^3$ up to >300 μg/m$^3$ as shown in Figure 5 and Figure 6. This declining trend of pH is not favorable for the $HNO_3$ partitioning into the particle phase (Nah et al., 2018). However, a clear enhanced trend of molar ratio of particulate nitrate in the total nitrate as a function of NR-$PM_1$ mass concentration was observed correspondingly (as shown in Figure 5 and Figure 6). Therefore, in this case the increase of aerosol liquid water is more likely to be the driving factor of particulate nitrate formation compared to the influence of pH.

It is worth noting that a similar co-condensation effect between water vapor and semi-volatile organic components (Topping and McFiggans, 2012;Topping et al., 2013;Hu et al., 2018) could promote the haze formation as well, for which there may be some evidence in the current case. Such a co-condensation effect will lead to the enhancement of semi-volatile organic and inorganic (e.g., nitrate) material with the increasing RH in a developing haze. The associated water will favor partitioning of

both $HNO_3$ and semi-volatile organic materials to the particle phase depending on the organic solubility, providing a linkage between the development of increasing organic and inorganic particle mass.

### 3.3 The key role of liquid water on visibility degradation

Aerosol particles grow up in size as ambient RH increases, further enhances their extinction coefficient and impacts visibility (Zhao et al., 2019;Kuang et al., 2016). In this section, size-resolved extinction coefficient of aerosol particles was estimated, and the influences of liquid water on the extinction coefficient and visibility were quantitatively evaluated. As shown in Figure 7a, the total light extinction coefficient of dry and wet aerosol particles enhanced by a factor of 4.3 and 5.4, respectively, from the beginning to a fully-developed haze. Correspondingly, the calculated visibility without considering liquid water degraded significantly from ~10 km to less than 2 km within 48 hours during the marked 'haze period'. The contribution of aerosol associated water to visibility impairment was negligible in the beginning (2%), while it was significant (up to 24%) in the fully-developed haze (Figure 7b). This indicates that liquid water facilitated visibility degradation during haze development.

The influences of liquid water on visibility degradation varied with aerosol particle size. The size-resolved chemical composition data showed that the inorganic species, mainly particulate nitrate, were dominant components in the aerosol particles within the size range of 300~700 nm (Figure S3). Correspondingly, the particles in this size range contained most of the liquid water (50~80% of the total aerosol liquid water content of $PM_1$). According to discussion in Sec. 3.2, the mutual promotion effect between liquid water and particulate nitrate can promote their mass loading enhancement. Aerosol particles in this size range experienced the most significant enhancement of light extinction due to water

uptake (Figure 8a and 8b) and contributed 70~88% of the total extinction coefficient of the total NR-$PM_1$ (Figure S9). In conclude, the rapid particulate nitrate enhancement enhanced the aerosol extinction coefficient during haze developing, while the aerosol water uptake further enhanced the visibility degradation by increasing extinction coefficient and promoting particulate nitrate enhancement.

It is worth noting that the enhanced dimming effect will further shallower the planetary boundary layer (PBL), which, in turn, depresses the dilution of water vapor and particulate matter in the atmosphere, hence leads to a higher RH and aerosol particle mass loading (Tie et al., 2017). Such effect is beyond the scope of this study.

# 4 Conclusions and implication

In this study, we observed a particulate nitrate-dominated (up to 44% of non-refractory $PM_1$ mass concentration) particulate matter pollution episode, which is typical during winter haze in Beijing, China. A clear co-increase of aerosol particle liquid water and particulate nitrate was observed, demonstrating the mutual promotion between them via observation-based theoretical calculations.

As shown in Figure 9, the water uptake by hygroscopic aerosols increased the aerosol surface area and volume, enhancing the condensational loss of $N_2O_5$ over particles and favoring the thermodynamic equilibrium of $HNO_3$ into the particle phase under the supersaturated ambient $HNO_3$ and $NH_3$. The enhanced particulate nitrate from the above pathways increased the mass fraction of particulate nitrate, which had a lower deliquescence RH than sulfate and resulted in more water uptake at lower ambient RH (Kreidenweis and Asa-Awuku, 2014). Hence, the increased aerosol particle surface area and

volume concentrations due to water uptake, in turn facilitates particulate nitrate enhancement. Hence, a feedback loop between liquid water and particulate nitrate enhancement is built up. Therefore the enhanced particulate nitrate components can accelerate the feedback compared with sulfate-rich pollution over the NCP region in the past (Hu et al., 2016). This self-amplification can rapidly degrade air quality and halve visibility within one day. Our results highlight the importance of reducing the particulate nitrate and its precursors (e.g. $NO_x$) for mitigation of haze episodes in NCP region.

## Data availability

The observational dataset of the BEST-ONE campaign can be accessed through the corresponding author Z. Wu (zhijunwu@pku.edu.cn).

The E-AIM model can be accessed via http://www.aim.env.uea.ac.uk/aim/aim.php.

## Author contributions

Z.W., Y.W. and Y.C. conceived the study. Y.Z., M.H., and A.K.S developed BEST-ONE field campaign program. Y.W., Z.W., D.S., Z.D., S.H.S., R.S., G.I.G., P.S., T.H., K.L., L.Z., C.Z., A.K.S., Y.Z., and M.H. participated in this campaign and collected the dataset. Y.W. conducted aerosol particle liquid water calculation under guide of Y.B. and thermodynamic equilibrium of particulate ammonium nitrate under guidance of G.M. Y.C. calculated the uptake coefficient of $N_2O_5$, optical properties and visibility. Y.W. and Y.C. cowrite the manuscript with the inputs from all co-authors. Z.W., G.M., A.K.S., S.H.S., G.I.G., P.S., T.H., A.V., and A.W. proofread and help improve the manuscript. All authors discussed the results.

## Acknowledgement

This work is supported by the following projects: National Natural Science Foundation of China (41571130021, 41875149), Ministry of Science and Technology of the People's Republic of China (2016YFC0202801), German Federal Ministry of Education and Research (ID-CLAR). Y.W. acknowledges the support of the China Scholarship Council and The University of Manchester Joint Scholarship Programme. We thank Dr. Paul I. Williams for valuable advice on reaction constant of $HNO_3$ and $N_2O_5$.

## References

Anttila, T., Kiendler-Scharr, A., Tillmann, R., and Mentel, T. F.: On the Reactive Uptake of Gaseous Compounds by Organic-Coated Aqueous Aerosols: Theoretical Analysis and Application to the Heterogeneous Hydrolysis of N2O5, The Journal of Physical Chemistry A, 110, 10435-10443, 10.1021/jp062403c, 2006.

Barnard, J. C., Fast, J. D., Paredes-Miranda, G., Arnott, W. P., and Laskin, A.: Technical Note: Evaluation of the WRF-Chem "Aerosol Chemical to Aerosol Optical Properties" Module using data from the MILAGRO campaign, Atmos. Chem. Phys., 10, 7325-7340, 10.5194/acp-10-7325-2010, 2010.

Bian, Y., Zhao, C., Ma, N., Chen, J., and Xu, W.: A study of aerosol liquid water content based on hygroscopicity measurements at high relative humidity in the North China Plain, 6417-6426 pp., 2014.

Brown, S. S., Ryerson, T. B., Wollny, A. G., Brock, C. A., Peltier, R., Sullivan, A. P., Weber, R. J., Dubé, W. P., Trainer, M., Meagher, J. F., Fehsenfeld, F. C., and Ravishankara, A. R.: Variability in Nocturnal Nitrogen Oxide Processing and Its Role in Regional Air Quality, Science, 311, 67-70, 10.1126/science.1120120, 2006.

Calvert, J. G., Lazrus, A., Kok, G. L., Heikes, B. G., Walega, J. G., Lind, J., and Cantrell, C. A.: Chemical mechanisms of acid generation in the troposphere, Nature, 317, 27, 10.1038/317027a0, 1985.

Chang, W. L., Brown, S. S., Stutz, J., Middlebrook, A. M., Bahreini, R., Wagner, N. L., Dubé, W. P., Pollack, I. B., Ryerson, T. B., and Riemer, N.: Evaluating N2O5 heterogeneous hydrolysis parameterizations for CalNex 2010, Journal of Geophysical Research: Atmospheres, 121, 5051-5070, doi:10.1002/2015JD024737, 2016.

Chen, Y., Wild, O., Wang, Y., Ran, L., Teich, M., Größ, J., Wang, L., Spindler, G., Herrmann, H., van Pinxteren, D., McFiggans, G., and Wiedensohler, A.: The influence of impactor size cut-off shift caused by hygroscopic growth on particulate matter loading and composition measurements, Atmospheric Environment, 195, 141-148, https://doi.org/10.1016/j.atmosenv.2018.09.049, 2018a.

Chen, Y., Wolke, R., Ran, L., Birmili, W., Spindler, G., Schröder, W., Su, H., Cheng, Y., Tegen, I., and Wiedensohler, A.: A parameterization of the heterogeneous hydrolysis of N2O5 for mass-based aerosol models: improvement of particulate nitrate prediction, Atmos. Chem. Phys., 18, 673-689, 10.5194/acp-18-673-2018, 2018b.

Cheng, Y., Zheng, G., Wei, C., Mu, Q., Zheng, B., Wang, Z., Gao, M., Zhang, Q., He, K., Carmichael, G., Pöschl, U., and Su, H.: Reactive nitrogen chemistry in aerosol water as a source of sulfate during haze events in China, Science Advances, 2, 10.1126/sciadv.1601530, 2016.

Clegg, S. L., Brimblecombe, P., and Wexler, A. S.: Thermodynamic Model of the System H+−NH4+−SO42-−NO3-−H2O at Tropospheric Temperatures, The Journal of Physical Chemistry A, 102, 2137-2154, 10.1021/jp973042r, 1998.

de Foy, B., Lu, Z., and Streets, D. G.: Satellite NO2 retrievals suggest China has exceeded its NOx reduction goals from the twelfth Five-Year Plan, Scientific Reports, 6, 35912, 10.1038/srep35912 https://www.nature.com/articles/srep35912#supplementary-information, 2016.

DeCarlo, P. F., Kimmel, J. R., Trimborn, A., Northway, M. J., Jayne, J. T., Aiken, A. C., Gonin, M., Fuhrer, K., Horvath, T., Docherty, K. S., Worsnop, D. R., and Jimenez, J. L.: Field-Deployable, High-Resolution, Time-of-Flight Aerosol Mass Spectrometer, Analytical Chemistry, 78, 8281-8289, 10.1021/ac061249n, 2006.

Dong, H. B., Zeng, L. M., Hu, M., Wu, Y. S., Zhang, Y. H., Slanina, J., Zheng, M., Wang, Z. F., and Jansen, R.: Technical Note: The application of an improved gas and aerosol collector for ambient air pollutants in China, Atmos. Chem. Phys., 12, 10519-10533, 10.5194/acp-12-10519-2012, 2012.

Ervens, B., Turpin, B. J., and Weber, R. J.: Secondary organic aerosol formation in cloud droplets and aqueous particles (aqSOA): a review of laboratory, field and model studies, Atmos. Chem. Phys., 11, 11069-11102, 10.5194/acp-11-11069-2011, 2011.

Fitzgerald, J. W.: Dependence of the Supersaturation Spectrum of CCN on Aerosol Size Distribution and Composition, Journal of the Atmospheric Sciences, 30, 628-634, 10.1175/1520-0469(1973)030<0628:dotsso>2.0.co;2, 1973.

Fountoukis, C., and Nenes, A.: ISORROPIA II: a computationally efficient thermodynamic equilibrium model for K+;Ca2+;Mg2+;NH4+;Na+;SO42-;NO3-;Cl-;H2O aerosols, Atmos. Chem. Phys., 7, 4639-4659, 10.5194/acp-7-4639-2007, 2007.

Ge, B., Xu, X., Ma, Z., Pan, X., Wang, Z., Lin, W., Ouyang, B., Xu, D., Lee, J., Zheng, M., Ji, D., Sun, Y., Dong, H., Squires, F. A., Fu, P., and Wang, Z.: Role of Ammonia on the Feedback Between AWC and Inorganic Aerosol Formation During Heavy Pollution in the North China Plain, Earth and Space Science, 6, 1675-1693, 10.1029/2019ea000799, 2019.

Ge, X., He, Y., Sun, Y., Xu, J., Wang, J., Shen, Y., and Chen, M.: Characteristics and Formation Mechanisms of Fine Particulate Nitrate in Typical Urban Areas in China, Atmosphere, 8, 62, 2017.

Gen, M., Zhang, R., Huang, D. D., Li, Y., and Chan, C. K.: Heterogeneous SO2 Oxidation in Sulfate Formation by Photolysis of Particulate Nitrate, Environmental Science & Technology Letters, 6, 86-91, 10.1021/acs.estlett.8b00681, 2019a.

Gen, M., Zhang, R., Huang, D. D., Li, Y., and Chan, C. K.: Heterogeneous Oxidation of SO2 in Sulfate Production during Nitrate Photolysis at 300 nm: Effect of pH, Relative Humidity, Irradiation Intensity, and the Presence of Organic Compounds, Environmental Science & Technology, 53, 8757-8766, 10.1021/acs.est.9b01623, 2019b.

Guo, S., Hu, M., Zamora, M. L., Peng, J., Shang, D., Zheng, J., Du, Z., Wu, Z., Shao, M., Zeng, L., Molina, M. J., and Zhang, R.: Elucidating severe urban haze formation in China, Proceedings of the National Academy of Sciences, 111, 17373-17378, 10.1073/pnas.1419604111, 2014.

Gysel, M., Crosier, J., Topping, D. O., Whitehead, J. D., Bower, K. N., Cubison, M. J., Williams, P. I., Flynn, M. J., McFiggans, G. B., and Coe, H.: Closure study between chemical composition and hygroscopic growth of aerosol particles during TORCH2, Atmos. Chem. Phys., 7, 6131-6144, 10.5194/acp-7-6131-2007, 2007.

Gysel, M., McFiggans, G. B., and Coe, H.: Inversion of tandem differential mobility analyser (TDMA) measurements, Journal of Aerosol Science, 40, 134-151, https://doi.org/10.1016/j.jaerosci.2008.07.013, 2009.

Heintzenberg, J.: Fine particles in the global troposphere A review, Tellus B: Chemical and Physical Meteorology, 41, 149-160, 10.3402/tellusb.v41i2.15064, 1989.

Hu, D., Topping, D., and McFiggans, G.: Measured particle water uptake enhanced by co-condensing vapours, Atmos. Chem. Phys., 18, 14925-14937, 10.5194/acp-18-14925-2018, 2018.

Hu, W., Hu, M., Hu, W., Jimenez, J. L., Yuan, B., Chen, W., Wang, M., Wu, Y., Chen, C., Wang, Z., Peng, J., Zeng, L., and Shao, M.: Chemical composition, sources, and aging process of submicron aerosols in Beijing: Contrast between summer and winter, Journal of Geophysical Research: Atmospheres, 121, 1955-1977, doi:10.1002/2015JD024020, 2016.

Hu, W., Hu, M., Hu, W. W., Zheng, J., Chen, C., Wu, Y., and Guo, S.: Seasonal variations in high time-resolved chemical compositions, sources, and evolution of atmospheric submicron aerosols in the megacity Beijing, Atmos. Chem. Phys., 17, 9979-10000, 10.5194/acp-17-9979-2017, 2017.

Huang, R.-J., Zhang, Y., Bozzetti, C., Ho, K.-F., Cao, J.-J., Han, Y., Daellenbach, K. R., Slowik, J. G., Platt, S. M., Canonaco, F., Zotter, P., Wolf, R., Pieber, S. M., Bruns, E. A., Crippa, M., Ciarelli, G., Piazzalunga, A., Schwikowski, M., Abbaszade, G., Schnelle-Kreis, J., Zimmermann, R., An, Z., Szidat, S., Baltensperger, U., Haddad, I. E., and Prévôt, A. S. H.: High secondary aerosol contribution to particulate pollution during haze events in China, Nature, 514, 218, 10.1038/nature13774 https://www.nature.com/articles/nature13774#supplementary-information, 2014.

Huang, X. F., He, L. Y., Hu, M., Canagaratna, M. R., Sun, Y., Zhang, Q., Zhu, T., Xue, L., Zeng, L. W., Liu, X. G., Zhang, Y. H., Jayne, J. T., Ng, N. L., and Worsnop, D. R.: Highly time-resolved chemical characterization of atmospheric submicron particles during 2008 Beijing Olympic Games using an Aerodyne High-Resolution Aerosol Mass Spectrometer, Atmos. Chem. Phys., 10, 8933-8945, 10.5194/acp-10-8933-2010, 2010.

Jayne, J. T., Leard, D. C., Zhang, X., Davidovits, P., Smith, K. A., Kolb, C. E., and Worsnop, D. R.: Development of an Aerosol Mass Spectrometer for Size and Composition Analysis of Submicron Particles, Aerosol Science and Technology, 33, 49-70, 10.1080/027868200410840, 2000.

Jimenez, J. L., Jayne, J. T., Shi, Q., Kolb, C. E., Worsnop, D. R., Yourshaw, I., Seinfeld, J. H., Flagan, R. C., Zhang, X., Smith, K. A., Morris, J. W., and Davidovits, P.: Ambient aerosol sampling using the Aerodyne Aerosol Mass Spectrometer, Journal of Geophysical Research: Atmospheres, 108, doi:10.1029/2001JD001213, 2003.

Köhler, H.: The Nucleus in and the Growth of Hygroscopic Droplets., Transactions of the Faraday Society, 32, 1152-1161, 1936.

Kolb, C. E., Cox, R. A., Abbatt, J. P. D., Ammann, M., Davis, E. J., Donaldson, D. J., Garrett, B. C., George, C., Griffiths, P. T., Hanson, D. R., Kulmala, M., McFiggans, G., Pöschl, U., Riipinen, I., Rossi, M. J., Rudich, Y., Wagner, P. E., Winkler, P. M., Worsnop, D. R., and O' Dowd, C. D.: An overview of current issues in the uptake of atmospheric trace gases by aerosols and clouds, Atmos. Chem. Phys., 10, 10561-10605, 10.5194/acp-10-10561-2010, 2010.

Koop, T., Bookhold, J., Shiraiwa, M., and Poschl, U.: Glass transition and phase state of organic compounds: dependency on molecular properties and implications for secondary organic aerosols in the atmosphere, Physical Chemistry Chemical Physics, 13, 19238-19255, 10.1039/C1CP22617G, 2011.

Kreidenweis, S. M., and Asa-Awuku, A.: 5.13 - Aerosol Hygroscopicity: Particle Water Content and Its Role in Atmospheric Processes A2 - Turekian, Heinrich D. HollandKarl K, in: Treatise on Geochemistry (Second Edition), Elsevier, Oxford, 331-361, 2014.

Kuang, Y., Zhao, C. S., Ma, N., Liu, H. J., Bian, Y. X., Tao, J. C., and Hu, M.: Deliquescent phenomena of ambient aerosols on the North China Plain, Geophysical Research Letters, 43, 8744-8750, doi:10.1002/2016GL070273, 2016.

Kulmala, M., Laaksonen, A., Korhonen, P., Vesala, T., Ahonen, T., and Barrett, J. C.: The effect of atmospheric nitric acid vapor on cloud condensation nucleus activation, Journal of Geophysical Research: Atmospheres, 98, 22949-22958, 10.1029/93JD02070, 1993.

Li, C., McLinden, C., Fioletov, V., Krotkov, N., Carn, S., Joiner, J., Streets, D., He, H., Ren, X., Li, Z., and Dickerson, R. R.: India Is Overtaking China as the World's Largest Emitter of Anthropogenic Sulfur Dioxide, Scientific Reports, 7, 14304, 10.1038/s41598-017-14639-8, 2017a.

Li, H., Zhang, Q., Zheng, B., Chen, C., Wu, N., Guo, H., Zhang, Y., Zheng, Y., Li, X., and He, K.: Nitrate-driven urban haze pollution during summertime over the North China Plain, Atmos. Chem. Phys., 18, 5293-5306, 10.5194/acp-18-5293-2018, 2018.

Li, Y. J., Liu, P. F., Bergoend, C., Bateman, A. P., and Martin, S. T.: Rebounding hygroscopic inorganic aerosol particles: Liquids, gels, and hydrates, Aerosol Science and Technology, 51, 388-396, 10.1080/02786826.2016.1263384, 2017b.

Liu, B. Y. H., Pui, D. Y. H., Whitby, K. T., Kittelson, D. B., Kousaka, Y., and McKenzie, R. L.: The aerosol mobility chromatograph: A new detector for sulfuric acid aerosols, Atmospheric Environment (1967), 12, 99-104, https://doi.org/10.1016/0004-6981(78)90192-0, 1978.

Liu, M., Huang, X., Song, Y., Xu, T., Wang, S., Wu, Z., Hu, M., Zhang, L., Zhang, Q., Pan, Y., Liu, X., and Zhu, T.: Rapid SO2 emission reductions significantly increase tropospheric ammonia concentrations over the North China Plain, Atmos. Chem. Phys., 18, 17933-17943, 10.5194/acp-18-17933-2018, 2018.

Liu, Y., Wu, Z., Wang, Y., Xiao, Y., Gu, F., Zheng, J., Tan, T., Shang, D., Wu, Y., Zeng, L., Hu, M., Bateman, A. P., and Martin, S. T.: Submicrometer Particles Are in the Liquid State during Heavy Haze Episodes in the Urban Atmosphere of Beijing, China, Environmental Science & Technology Letters, 4, 427-432, 10.1021/acs.estlett.7b00352, 2017.

Lu, K., Fuchs, H., Hofzumahaus, A., Tan, Z., Wang, H., Zhang, L., Schmitt, S. H., Rohrer, F., Bohn, B., Broch, S., Dong, H., Gkatzelis, G. I., Hohaus, T., Holland, F., Li, X., Liu, Y., Liu, Y., Ma, X., Novelli, A., Schlag, P., Shao, M., Wu, Y., Wu, Z., Zeng, L., Hu, M., Kiendler-Scharr, A., Wahner, A., and Zhang, Y.: Fast Photochemistry in Wintertime Haze: Consequences for Pollution Mitigation Strategies, Environmental Science & Technology, 53, 10676-10684, 10.1021/acs.est.9b02422, 2019.

Maitland, G. C., Rigby, M., Smith, E. B., and Wakeham, W. A.: Intermolecular forces: their origin and determination., International series of monographs on chemistry 3, 1981.

Massling, A., Niedermeier, N., Hennig, T., Fors, E. O., Swietlicki, E., Ehn, M., Hämeri, K., Villani, P., Laj, P., Good, N., McFiggans, G., and Wiedensohler, A.: Results and recommendations from an intercomparison of six Hygroscopicity-TDMA systems, Atmos. Meas. Tech., 4, 485-497, 10.5194/amt-4-485-2011, 2011.

McFiggans, G., Artaxo, P., Baltensperger, U., Coe, H., Facchini, M. C., Feingold, G., Fuzzi, S., Gysel, M., Laaksonen, A., Lohmann, U., Mentel, T. F., Murphy, D. M., O'Dowd, C. D., Snider, J. R., and Weingartner, E.: The effect of physical and chemical aerosol properties on warm cloud droplet activation, Atmos. Chem. Phys., 6, 2593-2649, 10.5194/acp-6-2593-2006, 2006.

Middlebrook, A. M., Bahreini, R., Jimenez, J. L., and Canagaratna, M. R.: Evaluation of Composition-Dependent Collection Efficiencies for the Aerodyne Aerosol Mass Spectrometer using Field Data, Aerosol Science and Technology, 46, 258-271, 10.1080/02786826.2011.620041, 2012.

Mozurkewich, M., and Calvert, J. G.: Reaction probability of N2O5 on aqueous aerosols, Journal of Geophysical Research: Atmospheres, 93, 15889-15896, doi:10.1029/JD093iD12p15889, 1988.

Nah, T., Guo, H., Sullivan, A. P., Chen, Y., Tanner, D. J., Nenes, A., Russell, A., Ng, N. L., Huey, L. G., and Weber, R. J.: Characterization of aerosol composition, aerosol acidity, and organic acid partitioning at an agriculturally intensive rural southeastern US site, Atmos. Chem. Phys., 18, 11471-11491, 10.5194/acp-18-11471-2018, 2018.

Petters, M. D., and Kreidenweis, S. M.: A single parameter representation of hygroscopic growth and cloud condensation nucleus activity, Atmos. Chem. Phys., 7, 1961-1971, 10.5194/acp-7-1961-2007, 2007.

Petzold, A., and Schönlinner, M.: Multi-angle absorption photometry—a new method for the measurement of aerosol light absorption and atmospheric black carbon, Journal of Aerosol Science, 35, 421-441, https://doi.org/10.1016/j.jaerosci.2003.09.005, 2004.

Petzold, A., Ogren, J. A., Fiebig, M., Laj, P., Li, S. M., Baltensperger, U., Holzer-Popp, T., Kinne, S., Pappalardo, G., Sugimoto, N., Wehrli, C., Wiedensohler, A., and Zhang, X. Y.: Recommendations for reporting "black carbon" measurements, Atmos. Chem. Phys., 13, 8365-8379, 10.5194/acp-13-8365-2013, 2013.

Pfeifer, S., Müller, T., Weinhold, K., Zikova, N., Martins dos Santos, S., Marinoni, A., Bischof, O. F., Kykal, C., Ries, L., Meinhardt, F., Aalto, P., Mihalopoulos, N., and Wiedensohler, A.: Intercomparison of 15 aerodynamic particle size spectrometers (APS 3321): uncertainties in particle sizing and number size distribution, Atmos. Meas. Tech., 9, 1545-1551, 10.5194/amt-9-1545-2016, 2016.

Putaud, J.-P., Raes, F., Van Dingenen, R., Brüggemann, E., Facchini, M. C., Decesari, S., Fuzzi, S., Gehrig, R., Hüglin, C., Laj, P., Lorbeer, G., Maenhaut, W., Mihalopoulos, N., Müller, K., Querol, X., Rodriguez, S., Schneider, J., Spindler, G., Brink, H. t., Tørseth, K., and Wiedensohler, A.: A European aerosol phenomenology—2: chemical characteristics of particulate matter at kerbside, urban, rural and background sites in Europe, Atmospheric Environment, 38, 2579-2595, https://doi.org/10.1016/j.atmosenv.2004.01.041, 2004.

Schwartz, S. E.: Mass-Transport Considerations Pertinent to Aqueous Phase Reactions of Gases in Liquid-Water Clouds., Chemistry of Multiphase Atmospheric Systems, 6. Springer, Berlin, Heidelberg, 1986.

Seinfeld., J. H., and Pandis., S. N.: Atmospheric Chemistry and Physics: from air pollution to climate change, John wiley & Sons, INC, 2006.

Shiraiwa, M., Ammann, M., Koop, T., and Pöschl, U.: Gas uptake and chemical aging of semisolid organic aerosol particles, Proceedings of the National Academy of Sciences, 108, 11003-11008, 10.1073/pnas.1103045108, 2011.

Spindler, G., Müller, K., Brüggemann, E., Gnauk, T., and Herrmann, H.: Long-term size-segregated characterization of PM10, PM2.5, and PM1 at the IfT research station Melpitz downwind of Leipzig (Germany) using high and low-volume filter samplers, Atmospheric Environment, 38, 5333-5347, https://doi.org/10.1016/j.atmosenv.2003.12.047, 2004.

Sun, Y., Jiang, Q., Wang, Z., Fu, P., Li, J., Yang, T., and Yin, Y.: Investigation of the sources and evolution processes of severe haze pollution in Beijing in January 2013, Journal of Geophysical Research: Atmospheres, 119, 4380-4398, 10.1002/2014jd021641, 2014.

Sun, Y. L., Wang, Z. F., Du, W., Zhang, Q., Wang, Q. Q., Fu, P. Q., Pan, X. L., Li, J., Jayne, J., and Worsnop, D. R.: Long-term real-time measurements of aerosol particle composition in Beijing, China: seasonal variations, meteorological effects, and source analysis, Atmos. Chem. Phys., 15, 10149-10165, 10.5194/acp-15-10149-2015, 2015.

Swietlicki, E., Hansson, H. C., HÄMeri, K., Svenningsson, B., Massling, A., McFiggans, G., McMurry, P. H., PetÄJÄ, T., Tunved, P., Gysel, M., Topping, D., Weingartner, E., Baltensperger, U., Rissler, J., Wiedensohler, A., and Kulmala, M.: Hygroscopic properties of submicrometer atmospheric aerosol particles measured with H-TDMA instruments in various environments—a review, Tellus B, 60, 432-469, 10.1111/j.1600-0889.2008.00350.x, 2008.

Tan, Z., Rohrer, F., Lu, K., Ma, X., Bohn, B., Broch, S., Dong, H., Fuchs, H., Gkatzelis, G. I., Hofzumahaus, A., Holland, F., Li, X., Liu, Y., Liu, Y., Novelli, A., Shao, M., Wang, H., Wu, Y., Zeng, L., Hu, M., Kiendler-Scharr, A., Wahner, A., and Zhang, Y.: Wintertime photochemistry in Beijing: Observations of ROx radical concentrations in the North China Plain during the BEST-ONE campaign, Atmos. Chem. Phys. Discuss., 2018, 1-33, 10.5194/acp-2018-359, 2018.

Tie, X., Huang, R.-J., Cao, J., Zhang, Q., Cheng, Y., Su, H., Chang, D., Pöschl, U., Hoffmann, T., Dusek, U., Li, G., Worsnop, D. R., and O'Dowd, C. D.: Severe Pollution in China Amplified by Atmospheric Moisture, Scientific Reports, 7, 15760, 10.1038/s41598-017-15909-1, 2017.

Topping, D., Connolly, P., and McFiggans, G.: Cloud droplet number enhanced by co-condensation of organic vapours, Nature Geoscience, 6, 443, 10.1038/ngeo1809
https://www.nature.com/articles/ngeo1809#supplementary-information, 2013.

Topping, D. O., and McFiggans, G.: Tight coupling of particle size, number and composition in atmospheric cloud droplet activation, Atmos. Chem. Phys., 12, 3253-3260, 10.5194/acp-12-3253-2012, 2012.

Vu, T. V., Shi, Z., Cheng, J., Zhang, Q., He, K., Wang, S., and Harrison, R. M.: Assessing the impact of Clean Air Action Plan on Air Quality Trends in Beijing Megacity using a machine learning technique, Atmos. Chem. Phys. Discuss., 2019, 1-18, 10.5194/acp-2019-173, 2019.

Wang, G., Zhang, R., Gomez, M. E., Yang, L., Levy Zamora, M., Hu, M., Lin, Y., Peng, J., Guo, S., Meng, J., Li, J., Cheng, C., Hu, T., Ren, Y., Wang, Y., Gao, J., Cao, J., An, Z., Zhou, W., Li, G., Wang, J., Tian, P., Marrero-Ortiz, W., Secrest, J., Du, Z., Zheng, J., Shang, D., Zeng, L., Shao, M., Wang, W., Huang, Y., Wang, Y., Zhu, Y., Li, Y., Hu, J., Pan, B., Cai, L., Cheng, Y., Ji, Y., Zhang, F., Rosenfeld, D., Liss, P. S., Duce, R. A., Kolb, C. E., and Molina, M. J.: Persistent sulfate formation from London Fog to Chinese haze, Proceedings of the National Academy of Sciences, 113, 13630-13635, 10.1073/pnas.1616540113, 2016.

Wang, H., Lu, K., Chen, X., Zhu, Q., Chen, Q., Guo, S., Jiang, M., Li, X., Shang, D., Tan, Z., Wu, Y., Wu, Z., Zou, Q., Zheng, Y., Zeng, L., Zhu, T., Hu, M., and Zhang, Y.: High N2O5 Concentrations Observed in Urban Beijing: Implications of a Large Nitrate Formation Pathway, Environmental Science & Technology Letters, 4, 416-420, 10.1021/acs.estlett.7b00341, 2017.

Wang, Y., Wu, Z., Ma, N., Wu, Y., Zeng, L., Zhao, C., and Wiedensohler, A.: Statistical analysis and parameterization of the hygroscopic growth of the sub-micrometer urban background aerosol in Beijing, Atmospheric Environment, 175, 184-191, https://doi.org/10.1016/j.atmosenv.2017.12.003, 2018.

Wang, Y., and Chen, Y.: Significant Climate Impact of Highly Hygroscopic Atmospheric Aerosols in Delhi, India, Geophysical Research Letters, 0, 10.1029/2019gl082339, 2019.

Wiedensohler, A., Birmili, W., Nowak, A., Sonntag, A., Weinhold, K., Merkel, M., Wehner, B., Tuch, T., Pfeifer, S., Fiebig, M., Fjäraa, A. M., Asmi, E., Sellegri, K., Depuy, R., Venzac, H., Villani, P., Laj, P., Aalto, P., Ogren, J. A., Swietlicki, E., Williams, P., Roldin, P., Quincey, P., Hüglin, C., Fierz-Schmidhauser, R., Gysel, M., Weingartner, E., Riccobono, F., Santos, S., Grüning, C., Faloon, K., Beddows, D., Harrison, R., Monahan, C., Jennings, S. G., O'Dowd, C. D., Marinoni, A., Horn, H. G., Keck, L., Jiang, J., Scheckman, J., McMurry, P. H., Deng, Z., Zhao, C. S., Moerman, M., Henzing, B., de Leeuw, G., Löschau, G., and Bastian, S.: Mobility particle size spectrometers: harmonization of technical standards and data structure to facilitate high quality long-term observations of atmospheric particle number size distributions, Atmos. Meas. Tech., 5, 657-685, 10.5194/amt-5-657-2012, 2012.

Wu, Z., Hu, M., Lin, P., Liu, S., Wehner, B., and Wiedensohler, A.: Particle number size distribution in the urban atmosphere of Beijing, China, 7967-7980 pp., 2008.

Wu, Z., Wang, Y., Tan, T., Zhu, Y., Li, M., Shang, D., Wang, H., Lu, K., Guo, S., Zeng, L., and Zhang, Y.: Aerosol Liquid Water Driven by Anthropogenic Inorganic Salts: Implying Its Key Role in Haze Formation over the North China Plain, Environmental Science & Technology Letters, 5, 160-166, 10.1021/acs.estlett.8b00021, 2018.

Wu, Z. J., Nowak, A., Poulain, L., Herrmann, H., and Wiedensohler, A.: Hygroscopic behavior of atmospherically relevant water-soluble carboxylic salts and their influence on the water uptake of ammonium sulfate, Atmos. Chem. Phys., 11, 12617-12626, 10.5194/acp-11-12617-2011, 2011.

Wu, Z. J., Zheng, J., Shang, D. J., Du, Z. F., Wu, Y. S., Zeng, L. M., Wiedensohler, A., and Hu, M.: Particle hygroscopicity and its link to chemical composition in the urban atmosphere of Beijing, China, during summertime, Atmos. Chem. Phys., 16, 1123-1138, 10.5194/acp-16-1123-2016, 2016.

Xie, Y., Wang, G., Wang, X., Chen, J., Chen, Y., Tang, G., Wang, L., Ge, S., Xue, G., Wang, Y., and Gao, J.: Observation of nitrate dominant PM2.5 and particle pH elevation in urban Beijing during the winter of 2017, Atmos. Chem. Phys. Discuss., 2019, 1-25, 10.5194/acp-2019-541, 2019.

Xu, Q., Wang, S., Jiang, J., Bhattarai, N., Li, X., Chang, X., Qiu, X., Zheng, M., Hua, Y., and Hao, J.: Nitrate dominates the chemical composition of PM2.5 during haze event in Beijing, China, Science of The Total Environment, 689, 1293-1303, https://doi.org/10.1016/j.scitotenv.2019.06.294, 2019a.

Xu, W., Sun, Y., Wang, Q., Zhao, J., Wang, J., Ge, X., Xie, C., Zhou, W., Du, W., Li, J., Fu, P., Wang, Z., Worsnop, D. R., and Coe, H.: Changes in Aerosol Chemistry From 2014 to 2016 in Winter in Beijing: Insights From High-Resolution Aerosol Mass Spectrometry, Journal of Geophysical Research: Atmospheres, 124, 1132-1147, 10.1029/2018jd029245, 2019b.

Yu, F., Luo, G.: Simulation of particle size distribution with a global aerosol model: contribution of nucleation to aerosol and CCN number concentrations, Atmos. Chem. Phys., 9, 7691-7710, 10.5194/acp-9-7691-2009, 2009.

Yue, F., Xie, Z., Zhang, P., Song, S., He, P., Liu, C., Wang, L., Yu, X., and Kang, H.: The role of sulfate and its corresponding S(IV)+NO2 formation pathway during the evolution of haze in Beijing, Science of The Total Environment, 687, 741-751, https://doi.org/10.1016/j.scitotenv.2019.06.096, 2019.

Yun, H., Wang, W., Wang, T., Xia, M., Yu, C., Wang, Z., Poon, S. C. N., Yue, D., and Zhou, Y.: Nitrate formation from heterogeneous uptake of dinitrogen pentoxide during a severe winter haze in southern China, Atmos. Chem. Phys., 18, 17515-17527, 10.5194/acp-18-17515-2018, 2018.

Zhang, R., Jing, J., Tao, J., Hsu, S. C., Wang, G., Cao, J., Lee, C. S. L., Zhu, L., Chen, Z., Zhao, Y., and Shen, Z.: Chemical characterization and source apportionment of PM2.5 in Beijing: seasonal perspective, Atmos. Chem. Phys., 13, 7053-7074, 10.5194/acp-13-7053-2013, 2013.

Zhao, C., Yu, Y., Kuang, Y., Tao, J., and Zhao, G.: Recent Progress of Aerosol Light-scattering Enhancement Factor Studies in China, Advances in Atmospheric Sciences, 36, 1015-1026, 10.1007/s00376-019-8248-1, 2019.

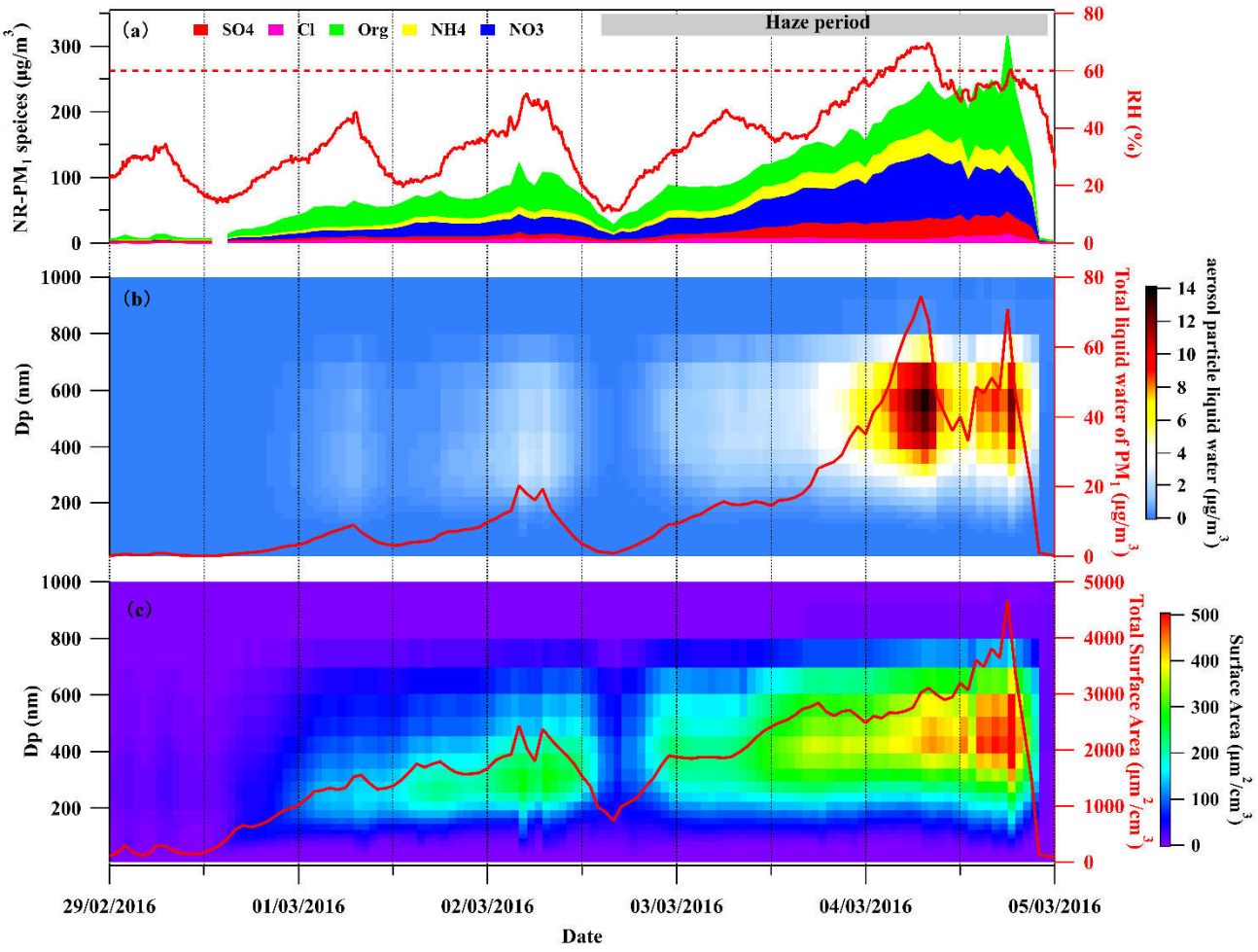


**Figure 1: The time series of (a) NR-PM$_1$ chemical composition measured by the HR-ToF-AMS and ambient RH (red solid line), (b) size-segregated aerosol particle liquid water and the total mass concentration of liquid water with smaller than 1 μm in aerodynamic diameter (red solid line), (c) size-segregated aerosol particle surface area and total aerosol particle surface area without considering particle hygroscopic growth during February 29 to March 5, 2016.**

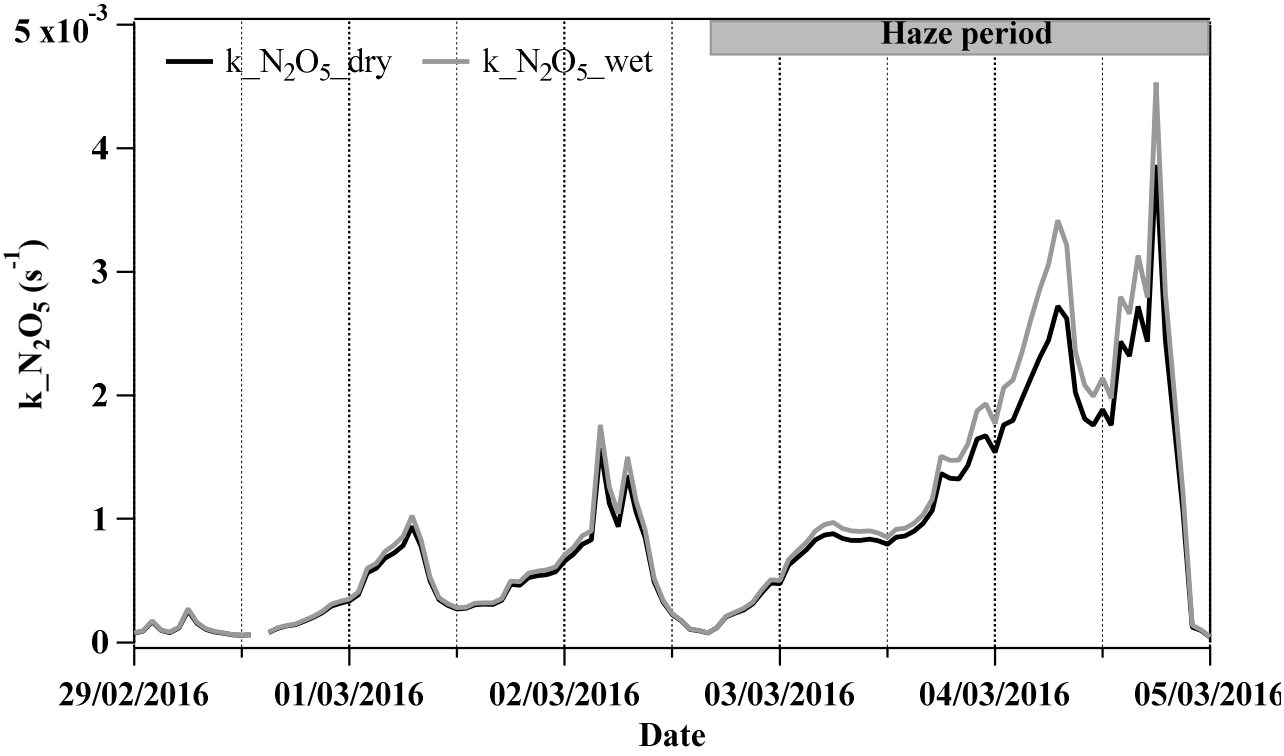


**Figure 2: The time series of condensational loss rate of $N_2O_5$ ($k\_N_2O_5$) with the calculation of dry particle number size distribution (PNSD) and wet PNSD during February 29 to March 5, 2016.**

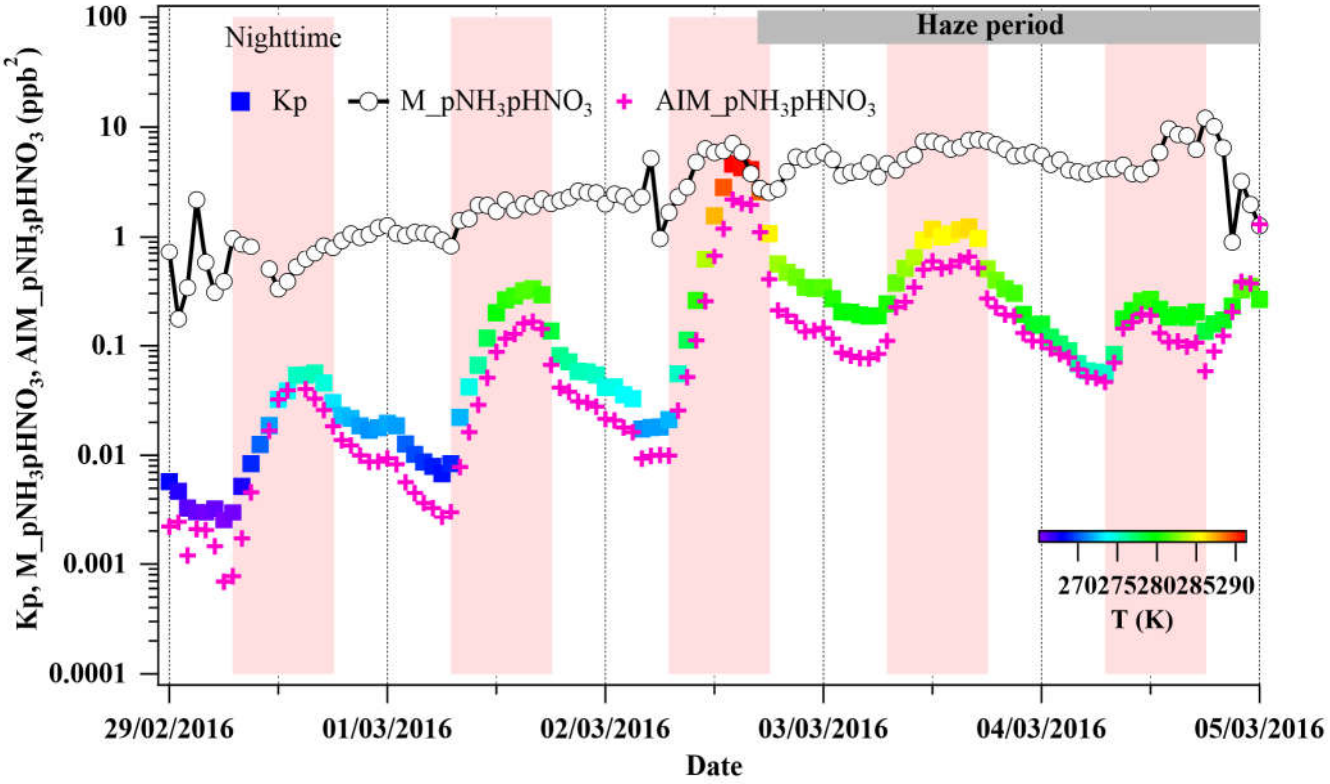


**Figure 3: The comparison of the calculated temperature-dependent dissociation constant of $NH_4NO_3$ (Kp) (Seinfeld. and Pandis., 2006) in the absence of liquid water, the product of equilibrium vapor pressure of gaseous $NH_3$ and $HNO_3$ from E-AIM ($AIM\_pNH_3pHNO_3$), and the product of mixing ratios of gaseous $NH_3$ and $HNO_3$ measured by GAC-IC ($M\_pNH_3pHNO_3$). Here, Kp is colored by the ambient temperature ranging 265~293K during February 29 to March 5, 2016.**

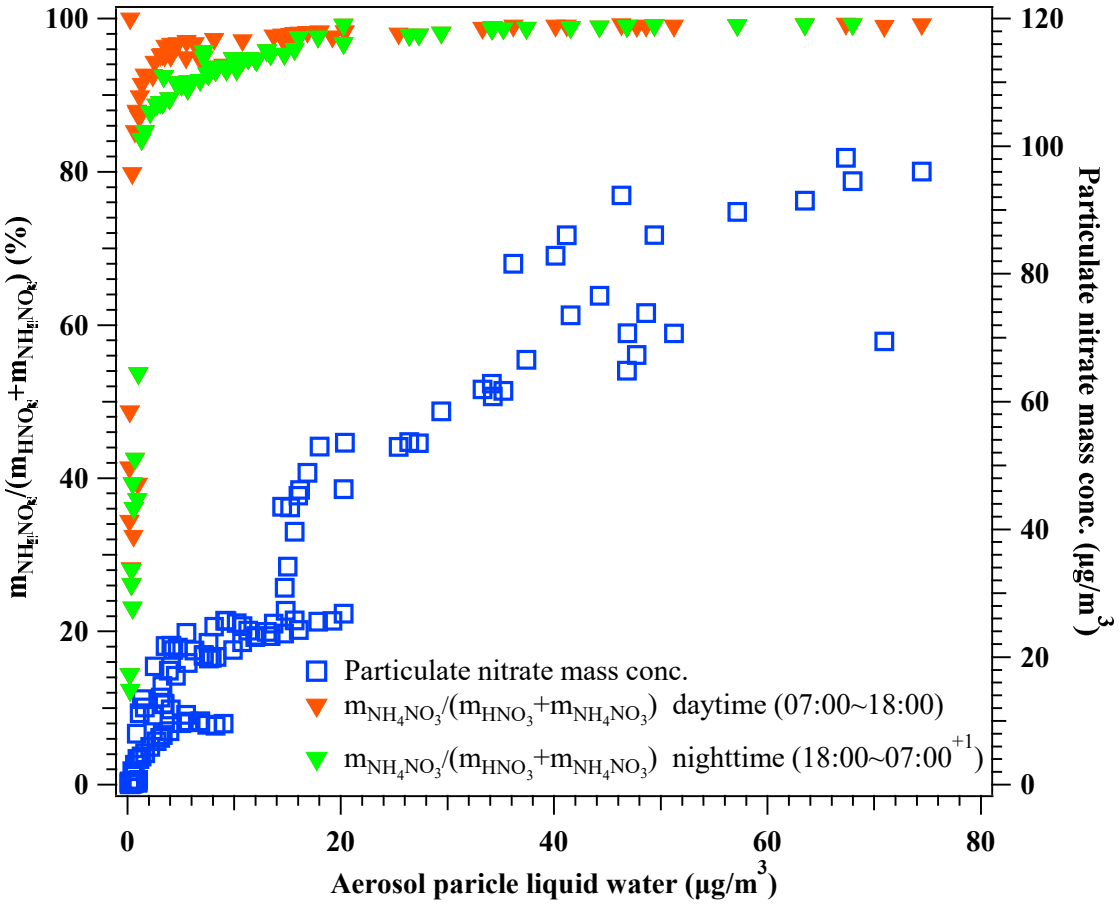


**Figure 4: The relationship between aerosol particle liquid water and the molar ratio of particulate nitrate in the total nitrate, $m_{NH_4NO_3}/(m_{HNO_3}+m_{NH_4NO_3})$ (left axis) during the nighttime 18:00~07:00+1 (green solid triangle) and the daytime at 07:00 ~ 18:00 (red solid triangle), and mass concentration of particulate nitrate as a function of aerosol liquid water (right axis) during the period of during February 29 to March 5, 2016. Here, particulate nitrate was measured by HR-ToF-AMS and the $HNO_3$ in the gas phase was measured by GAC-IC. Aerosol liquid water was calculated by H-TDMA-derived method.**

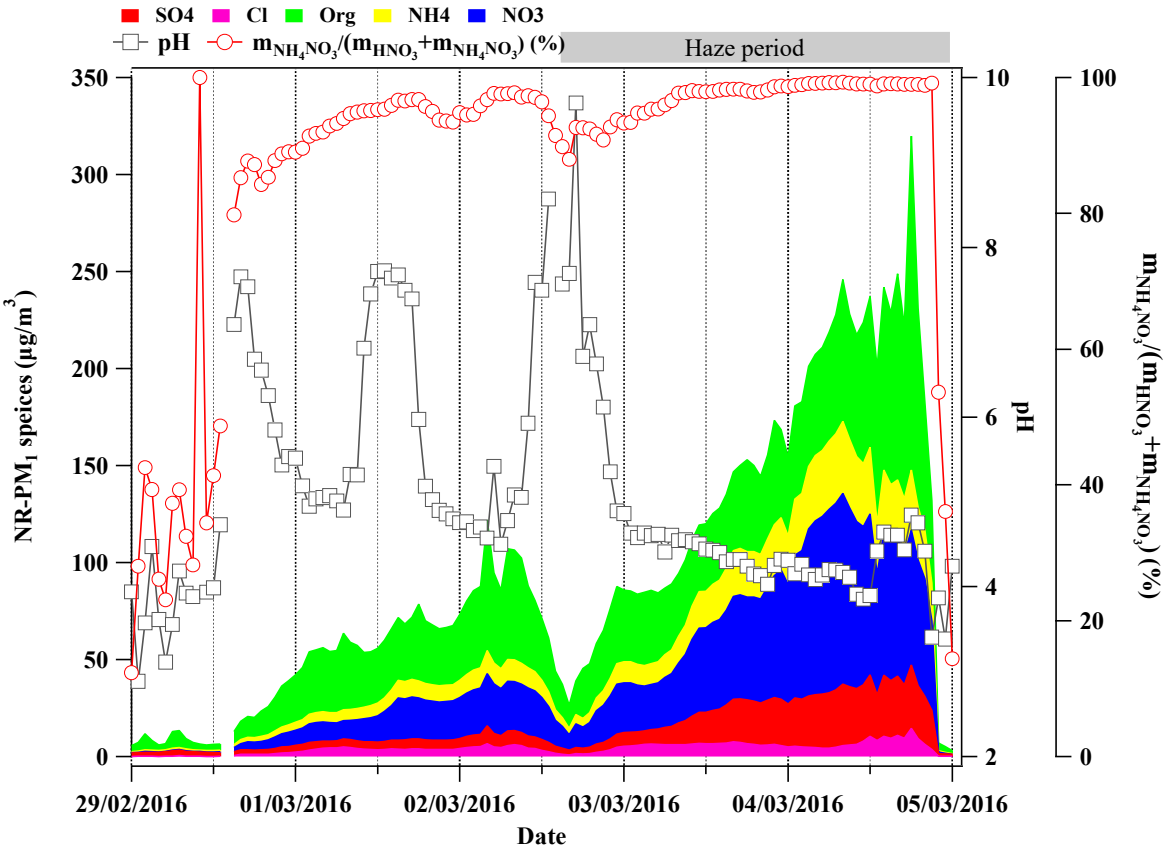


**Figure 5. The time series of chemical composition measured by HR-ToF-AMS (left axis), calculated aerosol pH by ISORROPIA II (inner right axis) and molar ratio of particulate nitrate in the total nitrate (gas+particle phase) shown on outer right axis during February 29 to March 5, 2016.**

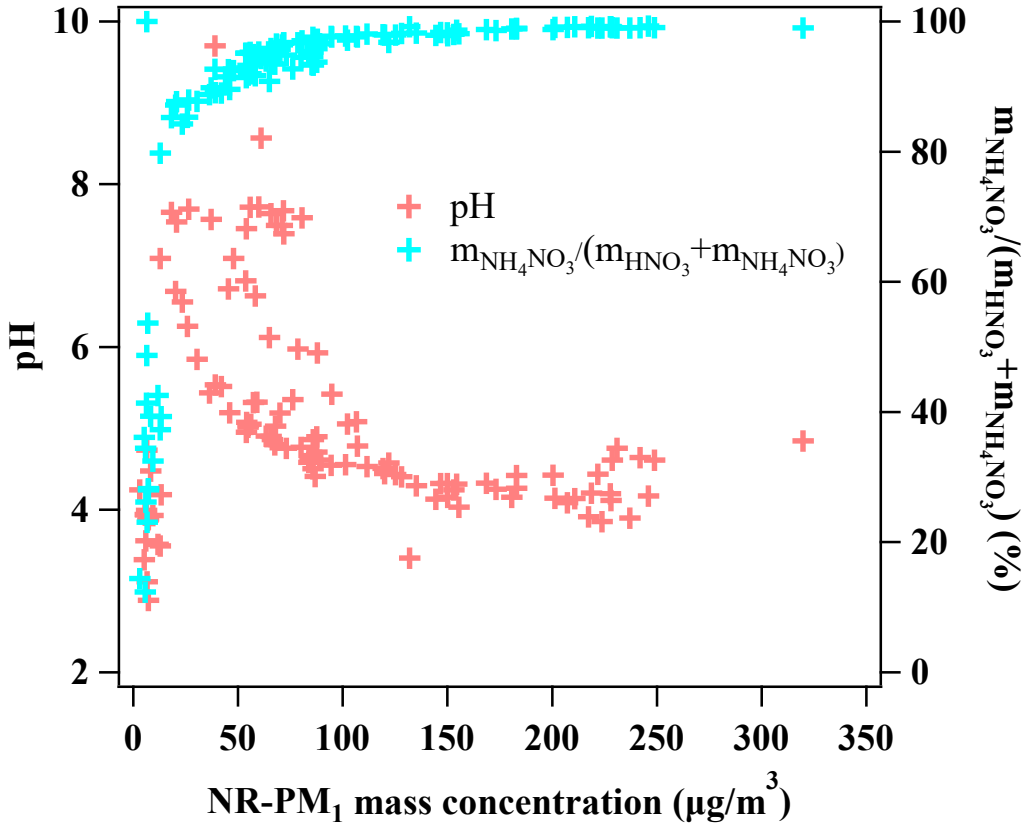


**Figure 6. The pH of the fine aerosol particles (left axis) and the molar ratio of particulate nitrate in the total nitrate (gas+particle phase) (right axis) as a function of NR-$PM_1$ mass concentrations.**

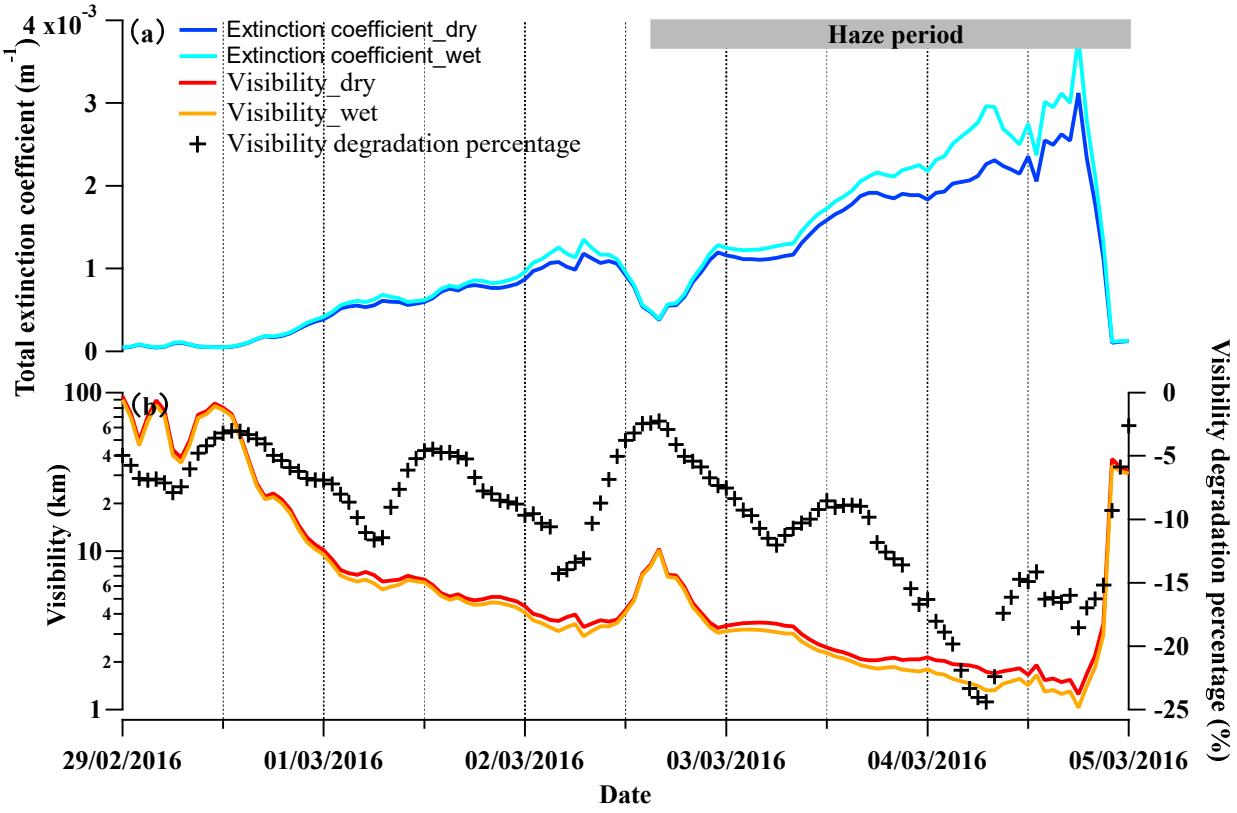


675

**Figure 7: The time series of (a) calculated total extinction coefficient at wavelength of 550 nm with the consideration of dry and wet PNSD, referred as Extinction coefficient_dry and Extinction coefficient_wet, (b) calculated visibility with the consideration of dry and wet PNSD, referred as Visibility_dry and Visibility_wet, respectively during February 29 to March 5, 2016. Visibility**

680 **degradation percentage is (Visibility_wet-Visibility_dry)/Visibility_dry, representing the visibility degradation in the presence of liquid water.**

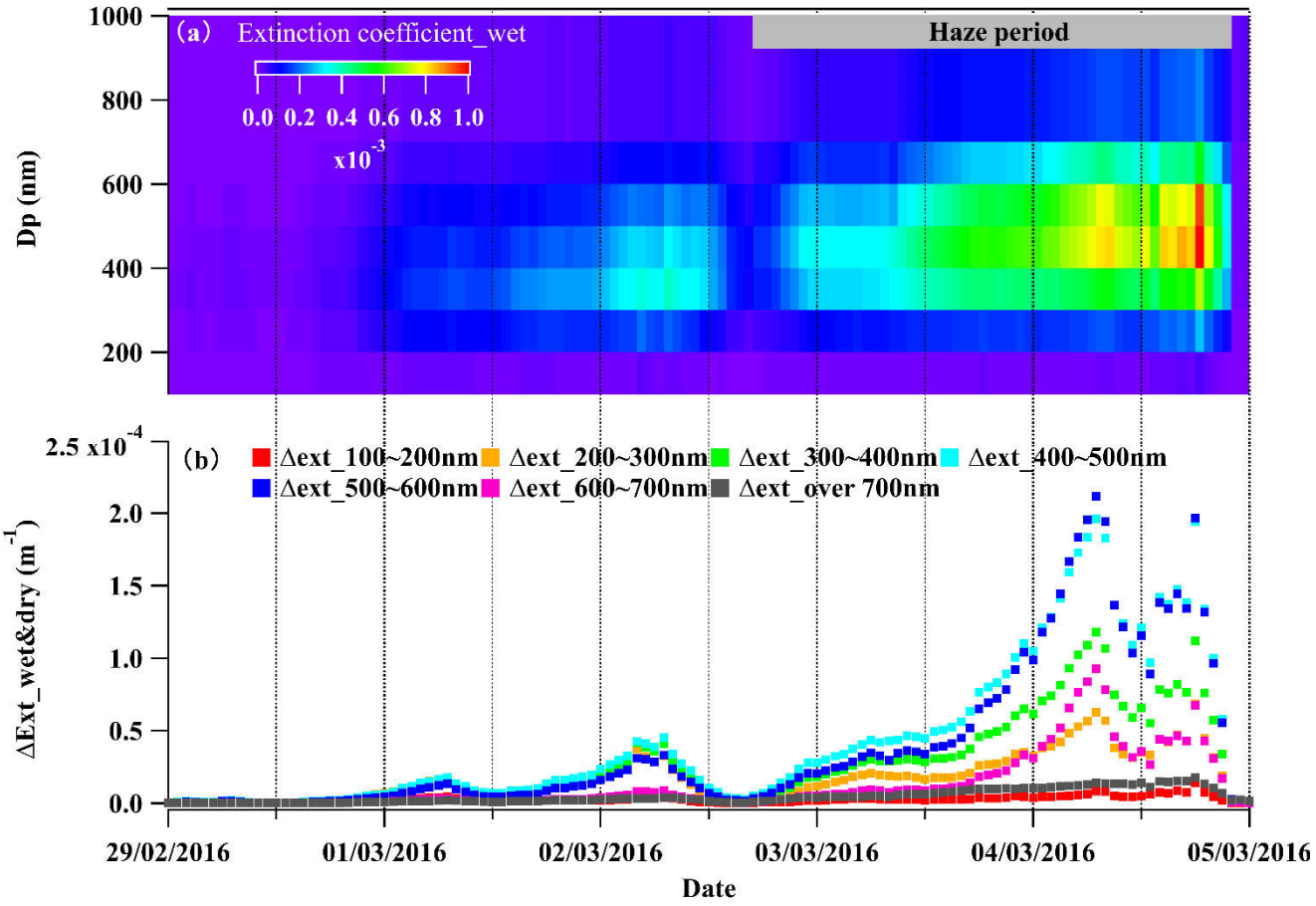


**Figure 8: (a) Size-segregated light extinction coefficient at wavelength of 550 nm for wet particles (Extinction coefficient_wet), (b) size-segregated difference between Extinction coefficient_wet and Extinction coefficient_dry, representing light extinction coefficient difference with and without considering liquid water during February 29 to March 5, 2016.**

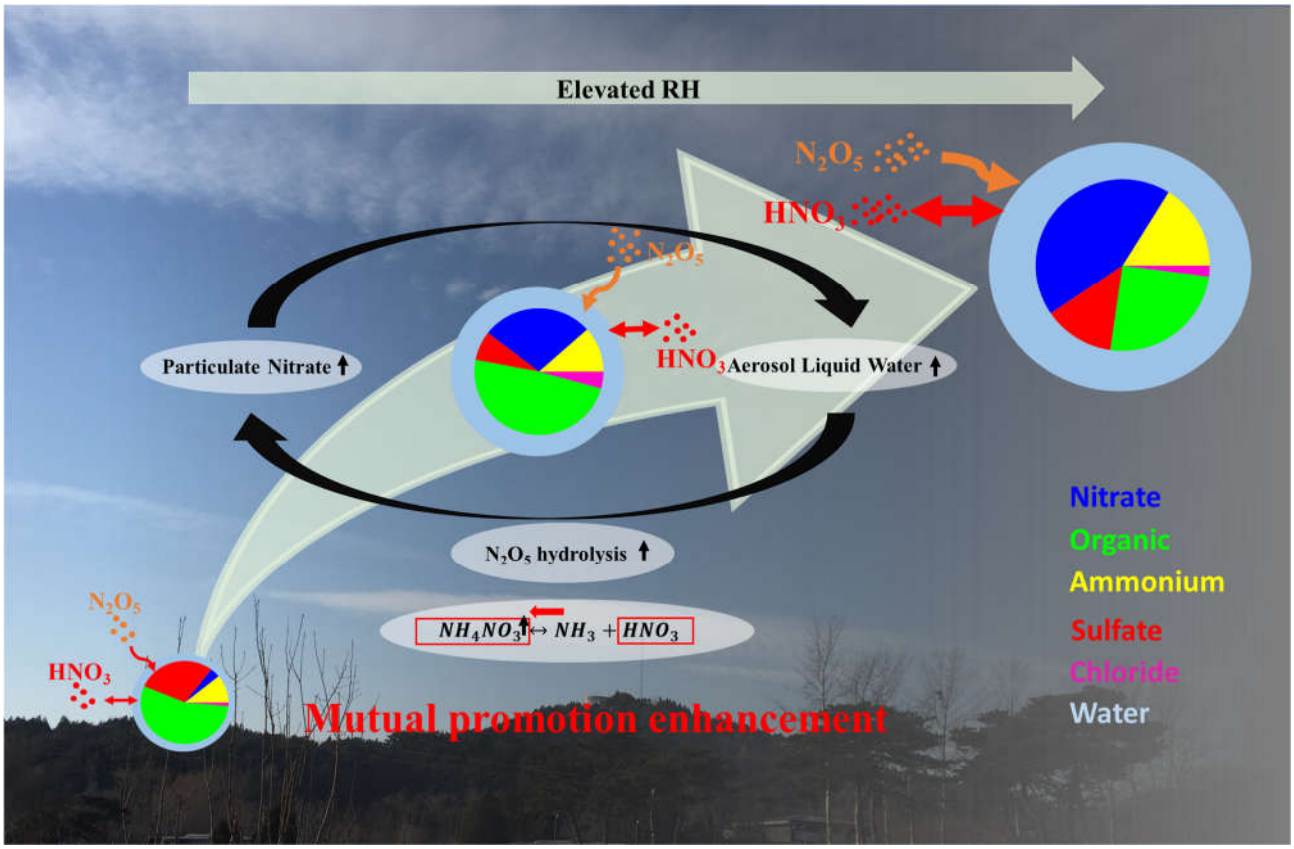


**Figure 9: The scheme of the mutual promotion effect between aerosol liquid water and particulate nitrate**